Microbial community of the deep-sea brine Lake Kryos seawater-brine interface is active below the chaotropicity limit of life as revealed by recovery of mRNA

Yakimov, M. M., La Cono, V., Spada, G. L., Bortoluzzi, G., Messina, E., Smedile, F., ... Giuliano, L. (2015). Microbial community of the deep-sea brine Lake Kryos seawater-brine interface is active below the chaotropicity limit of life as revealed by recovery of mRNA. Environmental Microbiology, 17(2), 364-382. DOI: 10.1111/1462-2920.12587

Published in:
Environmental Microbiology

Document Version:
Peer reviewed version

Received date: 06/06/2014

Accepted date: 07/31/2014

Research Article for EMI Special Issue: *Microbiology of low water-activity habitats*. Subtopic: *Microbial diversity/community genomics of hypersaline systems.*

Microbial community of the deep-sea brine Lake *Kryos* seawater-brine interface is active below the chaotropicity limit of life as revealed by recovery of mRNA.

Michail M. Yakimov[1,‡,*], Violetta La Cono,[1,‡] Gina La Spada,[1] Giovanni Bortoluzzi,[2] Enzo Messina,[1] Francesco Smedile,[1] Erika Arcadi,[1] Mireno Borghini,[3] Manuel Ferrer,[4] Phillippe Schmitt-Kopplin,[5,6] Norbert Hertkorn,[5] Jonathan A. Cray,[7] John E. Hallsworth,[7] Peter N. Golyshin,[8] and Laura Giuliano,[1,9]

[1] *Institute for Coastal Marine Environment, CNR, Spianata S.Raineri 86, 98122 Messina, Italy.*
[2] *Institute for Marine Sciences, CNR, Via Gobetti 101, 40129 Bologna, Italy.*
[3] *Institute for Marine Sciences, CNR Forte S.Teresa, 19136 Pozzuolo di Lerici, La Spezia, Italy.*
[4] *Institute of Catalysis, CSIC, Marie Curie 2, 28049 Madrid, Spain.*
[5] *Analytical BioGeoChemistry, Helmholtz Zentrum München, German Research Center for Environmental Health, Neuherberg, Germany.*
[6] *Analytical Food Chemistry, Technische Universität München, Freising-Weihenstephan, Germany.*
[7] *Institute for Global Food Security, School of Biological Sciences, MBC, Queen's University Belfast, BT9 7BL, Northern Ireland.*
[8] *School of Biological Sciences, Bangor University, Bangor, Gwynedd LL57 2UW, UK.*
[9] *Mediterranean Science Commission (CIESM), 16 bd de Suisse, MC 98000, Monaco.*

* Corresponding author

‡ These authors contribute equally to this work.

Running title: Prokaryotes within the interface of deep-sea Lake *Kryos*

This article has been accepted for publication and undergone full peer review but has not been through the copyediting, typesetting, pagination and proofreading process, which may lead to differences between this version and the Version of Record. Please cite this article as doi: 10.1111/1462-2920.12587

Key words: Messinian evaporites, Deep-sea anoxic brine lakes, Halophiles, Limits of life, Chaotropicity, Habitability, Mars

Summary

Within the complex of deep, hypersaline anoxic lakes (DHALs) of the Mediterranean Ridge we identified a new, unexplored DHAL and named it "Lake *Kryos*" after a nearby depression. This lake is filled with $MgCl_2$-rich, athalassohaline brine (salinity >470 practical salinity units), presumably formed by the dissolution of Messinian bischofite. Compared to the DHAL *Discovery*, it contains elevated concentrations of kosmotropic sodium and sulfate ions, which are capable of reducing the net chaotropicily of $MgCl_2$-rich solutions. The brine of Lake *Kryos* may therefore be biologically permissive at $MgCl_2$ concentrations previously considered incompatible with life. We characterized the microbiology of the seawater-*Kryos* brine interface and managed to recover mRNA from the 2.27-3.03 M $MgCl_2$ layer (equivalent to 0.747-0.631 water-activity) thereby expanding the established chaotropicity window-for-life. The primary bacterial taxa present there were KB1 candidate division and DHAL-specific group of organisms, distantly related to *Desulfohalobium*. Two euryarchaeal candidate divisions MSBL1 and HC1, detected in minority in the overlaying layers, accounted for more than 85% of the rRNA-containing archaeal clones analyzed in 2.27-3.03 M $MgCl_2$ layer. These findings shed light on the plausibility of life in highly chaotropic environments, geochemical windows for microbial extremophiles, and have implications for habitability elsewhere in the Solar System.

Introduction

In the eastern part of Mediterranean seafloor, an accretionary complex, named the Mediterranean Ridge, is formed by subduction of the African plate under the Eurasian and Anatolian plates. During the Messinian salinity crisis (late Miocene epoch, 5.33 - 5.96 million years ago) the repeated desiccations and re-fillings of the Mediterranean Sea resulted in the formation of enormous deposits of layered evaporites, that attain the thickness of up to 3.5 km in some places of eastern Mediterranean (Cita, 2006). In contrast to other tectonically active ridges, the deformational activity of the Mediterranean Ridge accompanied with presence of huge subsurface salt deposits appears to control the creation of peculiar submarine hydrological formations within confined depressions. The peculiar hydrology and chemistry of such lakes, which are named deep-sea hypersaline anoxic lakes (DHALs), discourages mixing of their brines with the overlying seawater (Raup, 1970). Seven such lakes, L'Atalante, Bannock, Discovery, Medee, Thetis, Tyro and Urania have been discovered and studied in the deep eastern Mediterranean over the last 20 years (De Lange and Ten Haven, 1983; MEDRIFF Consortium, 1995; Wallmann *et al.*, 1997; Chamot-Rooke *et al.*, 2005; La Cono *et al.*, 2011; Yakimov *et al.*, 2013). The surfaces of these brine lakes lie between 3.0 and 3.5 km below sea level and the salinity of their brines ranges from five to 13 times higher than that of seawater. Although these DHALs lie geographically close to each other (Fig. 1a), their hydrochemical diversity suggests that the processes leading to their formation were qualitatively different. As is generally accepted, during the desiccation/re-flooding cycles the salt deposition implied the simultaneous existence of early- and late-stage primary brines and evaporites. Seawater can be evaporated 10-fold without salt precipitation, resulting in formation of brine with salinity ≤330 PSU. This brine is named as "thalassohaline early-stage primary brine" (ESPB) and has proportions of all major ions characteristic to that of seawater. When the evaporation of seawater continues, salinity increases and the salts begin to precipitate changing the proportion of dissolved ions, thus forming the "athalassohaline Iate-stage primary brine" (LSPB). The insoluble calcium minerals precipitated first,

followed by precipitation of halite (NaCl), kieserite ($MgSO_4 \cdot KCl \cdot 3H_2O$), carnallite ($KMgCl_3 \cdot H_2O$), kainite ($MgSO_4 \cdot KCl \cdot 3H_2O$) and ending with formation of bischoffite ($MgCl_2 \cdot 6H_2O$), which is the most soluble of all marine evaporite salts (Wallmann *et al.*, 1997; Cita, 2006). Due to favorable climatic and geological conditions, both brines and solid stratified evaporite suites were stored in the subsurface for millions of years until tectonic activities would squeeze them on the seabed. For some Mediterranean DHALs, their idiosyncratic geomorphology implies the formation mechanisms other than simple outcropping of the Messinian evaporites followed by accumulation of high-density brines in the nearby depression. As has been proposed elsewhere, the evaporite dissolution could occur in sub-bottom deposits without direct exposure on the seafloor (Camerlenghi, 1990; Camerlenghi and McCoy, 1990; Cita, 1991, 2006). Tectonic activity in the Mediterranean Ridge leads to tensional stress and formation of seabed fractures and through these seawater can penetrate into deeper sediment layers ultimately reaching the subsurface layer of the Messinian evaporites. Osmotic pressure encourages movement of seawater towards the solid evaporites, dissolving the most soluble salts and increasing the volume of internal brine lenses. Notably, this movement of seawater is almost unidirectional, because the argillaceous Plio-Quaternary superficial sediments overlying the Messinian evaporites are "salt-rejecting", effectively behaving as a semipermeable membrane (Cita, 1991; 2006). Such continuing enrichment by evaporite dissolution leads to interstitial hydrologic formations, which in turn causes the overlying sediments to collapse and form a brine lake with characteristic confined, negative topography enriched by simple or complex morphologies ranging from sub-circular to elliptical, arc- or U-shaped basins, frequently including mounds and small, deeper depressions (Camerlenghi and McCoy, 1990).

Among all Mediterranean DHALs explored so far, only the *Discovery* Lake is filled with near-saturated $MgCl_2$-brine (5.05 M), suggesting that it derived via dissolution of bischofite, which is located within the uppermost layer of the evaporitic suite as explained above. Hence, the *Discovery* Lake is one of the saltiest athalassohaline water bodies on Earth (Table 1 and 2; Wallmann *et al.*,

1997, 2002). Due to the exceptionally high concentration of the divalent salt $MgCl_2$, this lake is approaching an anhydrous condition and is, simultaneously, an exceptionally chaotropic system with the lowest water activity (A_w) value registered for any hydrological formation on our planet (Marion *et al.*, 2003; Hallsworth *et al.*, 2007). In our previous study we demonstrated that exceptional chaotropicity of $MgCl_2$, rather than water activity reduction, is the window-of-life-determining parameter (Hallsworth *et al.*, 2007). We suggested that in the absence of compensating (e.g. kosmotropic) ions, such as sodium and sulfates, the upper concentration of $MgCl_2$, permissible for life, is about 2.3 M. This finding is consistent with the apparent $MgCl_2$ limit for microbial activity in the Dead Sea (Oren, 1999; 2010). As observed by Harrison *et al.* (2013), there have been relatively few studies on the way in which multiple stress parameters interact to determine the habitability of specific environments. A number of studies have, however, explored the way in which factors such as water activity, chaotropicity, nutrient availability and temperature can interact to determine biological permissivity of high-solute environments (Daffonchio *et al.*, 2006; Williams and Hallsworth, 2009; Chin *et al.*, 2010; Cray *et al.*, 2013a; 2013b; Lievens *et al.*, 2014).

Here, we present the results of the first oceanographic, geochemical and microbiological explorations of Lake *Kryos*, a second Mediterranean athalassohaline DHAL filled with nearly saturated $MgCl_2$-brine. Aside from slightly elevated concentrations of Na^+ and SO_4^{2-}, the hydrochemistry of this novel lake was found to share commonalities with that of the Lake *Discovery* (Table 1). As revealed by a comprehensive analysis of the vertical distribution of major prokaryotic groups along the seawater-brine interface, the *Kryos* prokaryotic community forms sharply stratified and dense ecosystem, operating at the very edge of Earth's biosphere. In order to decipher the stratification of principal metabolic pathways within this environment and, considering that DNA may be effectively conserved under highly chaotropic conditions, comparative analysis of recovered rRNA and mRNA transcripts were performed for three layers of the interface.

Results and discussion

Geomorphological and geochemical characterization of Lake Kryos*.*

During the cruise MIDDLE08 on RV *Urania* in September 2008, while on transit from the *Anoxic Lakes Region* West of Crete to the Lake *Medee,* we surveyed by 3.5 Chirp kHz swath-bathymetry profiling (SBP) confined depressions deeper than or similar to known seawater : DHAL interfaces (Fig. 1a). The candidate targets were localized by the morpho-bathymetric analysis of MEDIMAP data with resolution of 500 m (Loubrieu *et al.*, 2008). Given that the strong density contrast at the seawater-brine lake interface would have produced a straight line on acoustic swath bathymetrical profiling (SBP) data, we expected to be able to identify some yet unexplored DHALs. Approximately 20 nautical miles from the *Urania* Lake, we moved over a narrow North-South, elongated fracture (22°01'E 35°02'N – 22°02'E 34°53'N) and a sharp crisp line, hinting at the existence of a brine lake, was detected with maximum depth of about 3500 m. This was confirmed by direct conductivity-temperature-dissolved oxygen (CTD) profiling, brine sampling and bottom coring. Using the SBP data of the RV *Urania* DEEPPRESSURE cruise in 2013 and correcting the depths in the brines with the pressure data of the CTD casts, we obtained a map of the *Kryos* Lake with 20 to 25 m resolution. The Lake *Kryos* (named after the neighboring oxic depression) has the seawater-brine interface at 3387 dB (3337 m) and fills a steep, narrow basin approximately 18 km long and 1.7 km wide, oriented N-S and bending N-N-E at its northern tip with two arms oriented E-N-E (Fig. 1b). The bottom of the basin is 300-400 m below the depth of the surrounding region and has a well defined, continuous and very steep slope to the west, while in the opposite direction the seabed rises more moderately. The southern part of *Kryos* basin is characterized by several N-S oriented mounds and depressions,

presumably indicating the existence of isolated brine pools. Similar small pools may be detected at the northernmost part of the lake. Lake *Kryos*, including these small polar pools, has an area of about 100 km^2 and a volume of about 10 km^3. The central area of the lake is slightly deeper than 3500 m below sea level, implying that the depth of brine within the lake is approximately 160-170 m. The temperature measured at the seawater : brine interface was 13.98°C and slightly increased to 14.66°C within the brine, close to the seabed.

Chemical characterization of the *Kryos* brine revealed its extremely high salinity (471 g [kg H_2O]$^{-1}$) mainly due to extreme, close to saturation, concentration of Mg^{2+} (4.38 M) and Cl^- (9.04 M). As shown in the Table 1, the *Kryos* hydrochemistry is quiet similar to that of the *Discovery* brine with the exception of elevated concentrations of Na^+ and $SO4^{2-}$, which are present in the former. The *Kryos* basin is filled with almost 10 km^3 of $MgCl_2$-rich brine which compares to Lake *Discovery* volume of nearly 0.2 km^3 (Wallmann *et al.*, 1997, 2002); the DHAL *Kryos* is thus the largest deep-sea athalassohaline formation on Earth. Moreover, Lake *Discovery*, the $CaCl_2$–saturated *Don Juan Pond* and Lake *Kryos* together form a triad of the saltiest aquatic systems on our planet (Table 2). Previously made equilibrium calculations with the PHRQPITZ model (Wallmann *et al.*, 1997) have indicated that a LSPB similar in composition to those of the $MgCl_2$-rich athalassohaline brines may be produced when seawater is evaporated to the point of bischoffite precipitation, i.e. until only 5 g of initial 1000 g of H_2O remained in solution. A similar composition, termed as a secondary brine (SB), may also be formed when seawater is equilibrated with solid bischoffite and kainite ($K_4Mg_4Cl_4(SO_4)_4 \cdot 11H_2O$) (Table 2). Therefore, the major ion composition of both brine lakes is consistent with either a primary (evaporated seawater) or secondary origin (dissolution of the most soluble marine evaporite salts). As it generally accepted, concentrations of lithium could be used to differentiate between the primary and secondary brines, because this cation is conserved during seawater evaporation path and does not co-precipitate with evaporites in the presence of high Mg^{2+} concentrations (Carpenter, 1978; McCaffrey *et al.*, 1987; De Lange *et al.*, 1990; Wallmann *et al.*, 1997,

2002). By comparison with the LSPB values, lithium concentration in the *Discovery* and *Kryos* brines was 20-25 times less, indicating that both lakes have evidenced an extreme evaporation of the eastern Mediterranean, which is likely to have taken place during the late Messinian. As was proposed for Lake *Discovery*, the upmost layer of evaporite suite, represented by precipitated and lithium depleted bischoffite, was subsequently re-dissolved and has migrated to form a deep-sea brine pool. As it was shown by analysis of ^{4}He concentrations, before it entered the *Discovery* basin, the re-dissolved $MgCl_2$-saturated brine was initially stored for unknown period of time inside the sediments as interstitial brine pool (Wallmann *et al.*, 1997, 2002). We hypothesized that this scenario of the origin is equally applicable to the *Kryos* Lake.

The Kryos *and* Discovery *Lakes are the most chaotropic large-scale aquatic systems on Earth*

Earlier we have measured the water activities (A_w) in various $MgCl_2$–dominated solutions and evidenced that this salt is one of the most powerful A_w-reducing agents known (Hallsworth *et al.*, 2007); see also Winston and Bates (1960). Due to its high solubility and divalency, $MgCl_2$ is able to depress the water-activity values much below the limit observed for cell division or metabolic activity (Fig. 2a; Pitt, 1975; Marion *et al.*, 2003; Grant, 2004; Williams and Hallsworth, 2009). The water activity of saturated $MgCl_2$ is 0.340 in the range 10 - 15°C (Fig. 2a; Winston and Bates, 1960); we empirically determined the value for the *Discovery* brine; which was 0.382 A_w at 14.5°C (Hallsworth *et al.*, 2007). However, the established water-activity limit for (active) life (0.605[2]; Pitt and Christian, 1968) is equivalent to 3.7 M $MgCl_2$ (Hallsworth *et al.*, 2003a, 2007). The brine of *Kryos* contains a considerably higher concentration of $MgCl_2$ (4.38 M), which corresponds to 0.399 A_w. Another

[2] Whereas there have been a number of unsubstantiated claims of germination and growth of *Streptomyces* and *Micromonospora* strains at 0.500 A_w from one research group (Doroshenko *et al.*, 2005; 2006; Zvyagintsev *et al.*, 2007; 2009; 2012; Kurapova *et al.*, 2012), the limit for such Actinobacteria has recently been determined empirically at 0.890 A_w, with a theoretical lower limit which was derived by construction of isopleths growth profiles of approximately 0.870 A_w (Stevenson and Hallsworth, 2014).

harmful feature of $MgCl_2$–rich solutions, incompatible with existence of actively metabolizing organisms, is their exceptional chaotropicity (Hallsworth *et al.*, 2007; Cray *et al.*, 2013a), and it is this property, rather than any other activity of the solute, which can limit the microbial biosphere in high-$MgCl_2$ (and presumably other highly chaotropic) environments (Hallsworth *et al.*, 2007). Supporting this, our previous study on microbial communities of the *Discovery* Lake and recovery of unstable biomarkers, such as messenger RNA, suggested that in almost pure solutions of $MgCl_2$ representing the *Discovery* brine, the active life, as we currently know it, is not likely at $MgCl_2$ concentrations of > 2.3 M (Hallsworth *et al.*, 2007), which corresponds to < 0.790 A_w (Fig.2a). We are aware that the equation between these specific chaotropicity and water-activity values might be true only for the *Discovery* brine, almost depleted by sodium and sulfates. However, various sources of evidence suggest that this limit can also be expected for other habitats because chaotropes can to some extent be compensated by kosmotropes (Oren, 1983; Hallsworth *et al.*, 2003b, 2007; Williams and Hallsworth, 2009; Bhaganna *et al.*, 2010; Bell *et al.*, 2013), so the presence of other anions, like sodium and sulfate, can reduce the net chaotropicity of a hypersaline environment and widen the chaotropicity windows of life. Compared with the Lake *Discovery*, the Lake *Kryos* brine is slightly impoverished with $MgCl_2$ and simultaneously enriched with kosmotropic sodium and sulfate ions (Table 1), thus representing a unique opportunity to explore and test this assumption.

As shown in Figure 3, there is a sharp, ~2.5 m halocline at the seawater : brine lake interface characterized by a steep Mg^{2+} gradient ranging in concentration from 55 mM at its upper layer to 4.38 M in proximity to brine. Using our previous approach for A_w measurements of $MgCl_2$ solutions applied to *Discovery* samples (Hallsworth *et al.*, 2003b; 2007), we measured the A_w and chaotropicity levels of the *Kryos* interface (Fig. 2). The current window for chaotropicity equivalent (A_w = 0.790), established for the interface of *Discovery*, and the current window for xerophilic cellular life (A_w=0.605) embrace only upper two-thirds of the *Kryos* interface. An A_w value of 0.399 was determined for the *Kryos* brine itself and it is far below a minimal level of water activity, essential

for cellular function. The *Kryos* brine is thus an exceptionally chaotropic and low-water-activity environment, possibly the most large-scale, $MgCl_2$-saturated, aquatic system on Earth.

One year after the discovery of Lake *Kryos*, we begun exploring the extent to which cellular systems have been able to adapt to the *Kryos* interface conditions. Following this aim, the *Kryos* interface was sampled and fractionated using our previously established methodology to sample the DHAL interfaces (Daffonchio *et al.*, 2006; Borin *et al.*, 2009; Hallsworth *et al.*, 2007; Yakimov *et al.*, 2007a, 2007b, 2013; La Cono *et al.* 2011). Immediately after the rosette recovery, initial measurements of salinities of the bottommost content of Niskin bottles were performed. Obtained values were plotted over the reconstructed salinity profile (Fig. S1). We were aware that accurate capturing from elevated depths of *in situ* patterns of extremely unstable mRNA is potentially biased by changes in environmental conditions during the sample recovery (Feike *et al.*, 2012). To diminish this concern, all interface layers carrying similar biases, were sampled during the same cast and were processed in parallel. Due to the favorable weather conditions, little or no mixing had occurred during the sampling. Five Niskin bottles, exhibiting equivalent salinities at their bottoms, were used for further biological analyses (Fig. S1). Their contents were carefully fractionated anaerobically by slowly recovering 0.5-litre, 1-litre or 2-litre fractions from bottom tap. The subsamples collected from the bottommost part of these Niskin bottles (range of $MgCl_2$ 2.27 - 3.03 M) were pooled and hereafter termed as the AWW layer. As shown in Fig. 2a, the calculated A_w values for this layer (from 0.747 to 0.631) extend beyond both the established chaotropicity limit fro life[3] and close to the established water-activity limit for cell division of prokaryotes (for references, see Grant, 2004; Stevenson *et al.*, 2014). As anticipated, the presence of kosmotropic substances in the *Kryos* brine, such as sulfates, has a mitigating effect on the chaotropicity of $MgCl_2$ (Fig. 2b). For example, at ~0.760 A_w agar-gel point temperatures for both the *Kryos* brine and synthetic *Kryos* brine were ~6°C

[3] Based on the chaotropicity - A_w equivalence for the closest comparator brine, that of the *Discovery* lake (Hallsworth *et al.*, 2007).

higher than that of a $MgCl_2$ solution (Fig. 2b). This temperature difference is equivalent to a kosmotropicity of 25 kJ kg^{-1} (Hallsworth *et al.*, 2013a; Cray *et al.*, 2013a); the kosmotropic activity that is exerted by 2.3 M NaCl (Hallsworth *et al.*, 2007). The overlaying layer, hereafter termed CHW, had the range of $MgCl_2$ concentrations 1.30 – 2.27 M, corresponding to the established chaotropicity boundary (CHW) (Fig. S1), so the *Kryos* brine potentially represents habitable high-$MgCl_2$ environment thus far identified; equivalent to a chaotropicity of between 143 and 296 kJ kg^{-1} (Fig. S2). The upper interface (UIF) layer with salinity of 50-140 PSU was additionally analyzed to affirm the occurrence of stratified and metabolically active microbial populations thriving in deeper AWW and CHW compartments.

Characterization of dissolved organic matter in the Kryos *brine*

After dissolved organic matter (DOM) isolation by means of solid phase extraction, the desalted eluate was analyzed with ultrahigh resolution mass spectrometry (ion cyclotron resonance Fourier transform mass spectrometry, ICR-FT/MS) enabling a direct depiction of the DOM compositional space with a few thousands of assigned elemental formulas of this complex organic mixture. The mass spectra show a near Gaussian signal distribution typical of natural organic matter, with recognizable main mass spacings of methylene (Δm = 14.056 amu), double bond equivalents (DBE, Δm = 2.0157 amu) and a splitting of Δm = 0.0024 amu, denoting closely spaced CHO and CHOS compounds (Schmitt-Kopplin *et al.*, 2010a) indicative of a highly processed organic matter with appreciable extent of sulfurization at a relatively small overall molecular weight (<500 amu, Fig. 4a). Conversion of the signals into elemental compositions revealed a high abundance of sulfur compounds (700 CHOS and 250 CHNOS were assigned molecular formulas) reflecting the remarkable diverse sulfur chemistry in these particular extreme sulfide rich

environments (Fig. 4b,c). Neither organochlorines nor organomagnesium compounds were indicated by these datasets. The ratios of CHOS/CHO and CHNOS/CHNO molecular compositions in DOM were different, reflecting divergent mechanisms of sulfurization resulting in CHOS and CHNOS molecules. In contrast, purely abiotic reactivity of reactive sulfur species of presumably mineral origin with CHO and CHNO compounds led to comparable ratios (Schmitt-Kopplin *et al.*, 2010b). Hence, a biotic origin of the sulfur compounds observed in the *Kryos* brine seems highly likely. The van Krevelen diagrams show compounds with rather pronounced aliphaticity (elevated H/C ratio) and especially remarkable extent of oxygenation (O/C ratio > 0.6), extending even further than the previously described carboxyl-rich alicyclic materials (CRAM) (Fig. 4d). Further research is needed to elucidate the structural diversity of these compounds resembling the condensed alicyclic structures of biogenic origin such as sterols and hopanoids, which offer nominal unsaturation without overly abundance of sp^2 carbon (Hertkorn *et al.*, 2006).

Prokaryotic abundance and community composition of the Kryos *interface using CARD-FISH*

At the depth of ~3338 m, where the UIF *Kryos* sample was taken, total prokaryote number (DAPI-stained cells) increased six-fold compared to DAPI values for overlaying deep-sea water (Table 3). The number of cells in the CHW interface layer increased to $5.57 \pm 0.45 \times 10^5$ cell ml^{-1} and than gradually decreased to $2.47 \pm 0.11 \times 10^5$ cell ml^{-1} in the AWW layer, which was below the CHW. CARD-FISH indicated that while almost all DAPI-stained cells from the overlaying seawater contained 16S rRNA (89%), the numbers of CARD-positive microorganisms in the UIF interface layer dropped almost to a half of those visualized by DAPI (53 %). The gradual increase of CARD-positive fraction from 68 to 81% of all DAPI-stained cells was observed in deeper layers (Table 3). This phenomenon of increase in cell density likely reflects trapping and effective conservation under highly chaotropic conditions of stable biological macromolecules, such as DNA and rRNA, albeit in an inactivated form

(Duda *et al.*, 2004; Hallsworth *et al.*, 2007; Cray *et al.*, 2013a). Nevertheless, the existence of as-yet-undiscovered life forms, that have evolved greater chaotropicity and water activity tolerances than presently known, cannot be ruled out (Hallsworth *et al.*, 2007).

As revealed by taxon-specific CARD-FISH analysis (Table 3 and Table S1), bacteria dominated all studied layers of the *Kryos* interface. Previously we have shown that bacterial community thriving in the low interface of Lake *Discovery* was characterized by overwhelming dominance of members of KB1 candidate division and organisms, distantly related to *Desulfohalobium* (Hallsworth *et al.*, 2007). Application of KB1-specific FISH-probes (Yakimov *et al.*, 2013) revealed that, being absent in UIF community these extremely halophilic prokaryotes are gradually dominating the CHW and AWW populations. Distribution of DHAL-specific deltaproteobacteria was found be more homogeneous in both saltiest layers. Thaumarchaeota and Euryarchaeota exhibited opposing distribution patterns in relation to depth. The absolute dominance of Euryarchaeota in hypersaline and anoxic habitats is a characteristic feature for all currently studied DHALs interfaces (Daffonchio *et al.*, 2006; Borin *et al.*, 2009; Hallsworth *et al.*, 2007; Yakimov *et al.*, 2007a, 2007b, 2013; La Cono *et al.*, 2011). Noteworthy, below the established A_w-limit of life (0.605) the CARD-FISH analysis with the universal archaeal probe ARCH915 detected more than 40000 ribosome-containing cells ml^{-1}, whereas none of them were visualized there by more specific EURY806 probe (Table 3). This observation can be explained by the presence in the AWW samples of organisms, such as the members of MSBL1 candidate division, whose 16S rRNA sequences are out of the EURY806 probe specificity range.

Stratification of the Kryos *interface prokaryotic 16S rRNAs across the chaotropicity limit of life*

To survey the distribution of ribosome-containing Bacteria and Archaea, total RNA (50.42, 35.37 and 32.18 ng μl^{-1}) was respectively extracted from UIF, CHW and AWW samples. Total cDNA was further obtained by reverse transcription with hexa-random primers, PCR amplified with 16S rDNA-specific primers (Table S2), cloned and a total of 464 and 386 archaeal and bacterial inserts were partially sequenced. Phylogenetic analysis of the resulting reads revealed a pronounced stratification of prokaryotes thriving in the extremely chaotropic and salty compartments of the *Kryos* interface just above and below the established chaotropicity boundary of life (Fig. 5a). Remarkably, presence of layer-specific groups of 16S rRNA sequences in all three samples indicated that accurate fractionation of the *Kryos* interface was successful and reciprocal mixing had not occurred during recovery and subsequent processing of gradient samples. As for the overlaying deep seawater, members of Marine Group I Thaumarchaeota dominate the UIF archaeal community. In concordance with CARD-FISH analysis, ribosomal RNA-containing dormant thaumarchaeal cells have been settled in deeper interface compartment CHW from above layers, thus resulting in a significantly distorted indication of diversity of autochthonous metabolically active archaeal population. Two groups of halophilic Euryarchaeota, the MSBL1 and HC1 candidate divisions, detected in minority in the CHW layer, became dominant euryarchaeal groups in AWW layer, accounting for more than 85% of all archaeal clones (Fig. 5b). 16S rRNA sequences of extremely halophilic haloarchaea and methylotrophic methanogens, also being presented in CHW by singletons, were remainders of the AWW archaeal community. Remarkably, together with clones retrieved from the Lake *Discovery,* the MSBL1- and Halobacteriales-related *Kryos* clones formed separate clusters, which constitute evidence for the existence of $MgCl_2$-adapted species or genera within these candidate divisions (Fig. 6).

The empirically determined water-activity value for the 3.03 M $MgCl_2$ *Kryos* layer is 0.631, which is considerably close to the established limit for growth of halophilic prokaryotes (i.e.

~0.755; Grant, 2004). Recent studies, however, have demonstrated cell division of more than 10 halophilic prokaryotes, including members of the Halobacteriales in the range 0.717 to 0.6011 A_w (JE Hallsworth *et al.*, unpublished data) and the findings of the current study are consistent with their water-activity minima. These include empirically determined A_w values of 0.693 for *Halococcus salifodinae*, 0.687 for *Halobacterium noricense*, and 0.681 for *Natrinema pallidum* as well as values derived by extrapolation of 0.680 for *Halorhodospira halochloris*, 0.675-0.670 for halophilic bacteria belonging to the *Salinibacter* assemblage from crystallizer pond CR-30 (Braç del Port, Alicante), 0.668 for *Haloanaerobium lacusrosei*, 0.660 for *Actinopolyspora halophila*, 0.658 for *Halobacterium* strain 004.1, 0.647 for *Halorhabdus utahensis*, 0.623 for *Halorhodospira halophila*, 0.615 for *Halobacterium* strain GN-5, and 0.611 for *Halobacterium* strain GN-2.

Phylogenetic composition of the bacterial fraction recovered from all three analyzed layers is shown in Figure 5a and in Supplementary Material (Figure S3 and S4). Compared with the UIF and CHW 16S rRNA libraries, much lower diversity of bacterial phylotypes was recovered from the AWW layer of the *Kryos* interface. This included members of KB1 candidate division (54% of all clones sequenced) and yet unknown hyperhalophilic groups of the class Deltaproteobacteria (rest of the AWW clones) (Fig. 5b). Whereas coherent KB1-related organisms thrived also in the upper CHW layer, two phylogenetic clusters of Deltaproteobacteria, probably representing different extremely halophilic genera, were detected exclusively in the ultimate layer of the water-activity window for life (AWW) (Fig. 7). The less chaotropic and less salty CHW layer of the *Kryos* interface was inhabited by completely distinct population of Deltaproteobacteria, consisting of sulfate reducing bacteria (SRB) distantly related to the genera *Desulfotignum* and halophilic *Desulfosalsimonas* (Fig. 7). Noteworthy, all bacterial AWW phylogenetic groups have close relatives recovered from sediments of the Mediterranean solar salterns and surficial hypersaline lakes *Aran-Bidgol* (Iran) and *Tebenquiche* (Chile) (Demergasso

et al., 2008; Baati *et al.*, 2010; Makhdoumi-Kakhki *et al.*, 2012), thus considerably reducing the sampling efforts needed for their eventual culturing and the study of their physiology and metabolism.

As we have shown previously (Hallsworth *et al.*, 2007), bacterioplankton from overlaying compartments once entered by sedimentation in the sterile *Discovery* brine, is accumulating there at such highly conserved state that DNA from these organisms can be amplified. Consequently, DNA-based methodologies seem inaccurate approaches to study the "signatures of active life" under highly chaotropic conditions. Indeed, phylogenetic analysis of total DNA sampled at the depth of 3370 m revealed the occurrence in the *Kryos* brine of 16S rDNA signatures belonging to both Bacteria and Archaea dominating the deep-sea seawater and surficial layers of the interface, but missing in AWW layer (Figures 5a and S3-S5). Namely, almost 30% and 15% of all bacterial and archaeal clones recovered from the *Kryos* brine were respectively attributed to the Epsilonbacteria and Marine Group I Thaumarchaeota, the groups of prokaryotic organisms which dominated the UIF and CHW layers but were undetectable in the AWW layer. Similar distribution patterns, i.e. lack in AWW but occurrence in the *Kryos* brine, were observed for the members of Bacteroidetes, Gammaproteobacteria, Planctomycetes and archaeal candidate division SA1. None of brine-specific archaeal 16S rRNA sequences different from that of UIF, CHW and AWW libraries was detected in the *Kryos* brine, suggesting that all prokaryotic diversity detected in the *Kryos* brine derived from the overlaying deep seawater column and the interface. UniFrac PCA analysis affirmed that the microbial community of the *Kryos* interface exhibited notable stratification, mediated by a succession of different groups of organisms. Whereas being marginally different from the intermediate CHW layer ($P = 0.039$), the AWW bacterial population resulted statistically different from the less salty UIF sample ($P < 0.001$) (Fig. S6a). Consistently with the statement that the *Kryos* brine acts as a trap for descending allochthonous bacterioplankton, no statistical significant distance was found between BB (DNA-

based survey) and AWW layers; and only small difference was observed between BB and CHW layers (P = 0.033). The archaeal community behaved in similar manner, although the detected stratification was found to be less pronounced due to aforementioned influence of Marine Group I Thaumarchaeota. Both statistically allied AWW and BB layers resulted only slightly different form the UIF sample (corresponding P values of 0.12 and 0.18) and no statistical significant distances between the AWW, BB and CHW layers were detected (Fig. S6b).

Evidence that metabolic activity occurs in the AWW layer; i.e. below the established chaotropicity window for life

As mentioned above, the majority of the AWW archaeal community comprised of the MSBL1 and HC1 candidate divisions. Previously we speculated, that on basis of phylogenetic relatedness to methanogens and the lack of other groups that might be responsible of the detected methane production in some of Mediterranean DHALs, the MSBL1 members might be involved in methanogenesis at high salinity (van der Wielen *et al.*, 2005; Daffonchio *et al.*, 2006; Borin *et al.*, 2009; Yakimov *et al.*, 2013). Due to the fact that genetic determinants for methanogenesis in MSBL1 organisms remain unknown, we cannot examine their metabolic activities. Nevertheless, the phylogenetic lineage related to the genus *Methanohalophilus* was detected in AWW interface layer as considerable fraction of clones (5%), thus making feasible the assessment of their methanogenic activity via the recovery of alpha subunit of methylcoenzyme M reductase (*mcr*A) gene transcript. Unlike the *mcr*A diversity of the *Discovery* interface, where only *Methanohalophilus*-related sequences were detected (Hallsworth *et al.*, 2007), the *Kryos* interface possessed two distinct phylogenetic clusters of this gene (Fig. 5a). The CHW-specific *mcr*A group was found be distantly related to methylcoenzyme M reductase of *Methanomassiliicoccus*

luminyensis. This methylotrophic methanogenic *Thermoplasmata* archaeon carries a reduced methanogenesis pathway, restricted by reduction in the presence of H_2 of methanol and other methylated compounds to methane (Dridi *et al.*, 2012; Grolas *et al.*, 2012; Borrel *et al.*, 2013). Although this type of metabolism was never sought in the DHAL ecosystems, the eventual occurrence of this obligate H_2-dependent methylotrophic type of methanogenesis should be taken into account in future studies and cultivation attempts. Coherently with the *Discovery* *mcr*A gene expression survey, the diversity of the AWW *mcr*A transcripts was extremely low and all sequences were found be almost identical to that retrieved from the deepest, populated layer of the *Discovery* interface (2.23 M of $MgCl_2$) (Hallsworth *et al.*, 2007). This observation confirmed the assumption that the AWW layer of the *Kryos* interface is inhabited by a distinct archaeal population, which is able to thrive at high concentrations of Mg^{2+}.

The bacterial community of the AWW layer characterized by an extremely low diversity, with only two major taxa of hyperhalophilic organisms present. Similarly to MSBL1, lack of genomic information of the KB1 candidate division precludes any of metabolic gene expression surveys. However, the metabolic activity of sulfur reducing deltaproteobacteria in the AWW layer of the *Kryos* interface was indicated by the recovery and analysis of *dsrAB* gene transcripts. It is important to note that the AWW layer contained both the highest H_2S concentration and the number of SRBs-related sequences in all three layers analyzed, pointing out to an important ecological role of their members in the sulfur cycle of the *Kryos* ecosystem. This statement is also coherent with the analysis of DOM in the sterile *Kryos* brine, where the biotic sulfur compounds, obviously originated from the overlaying interface, were observed. The existence of hitherto unknown hyperhalophilic groups within SRBs was subsequently corroborated by the phylogenetic attribution of *dsrAB* gene transcripts recovered from the AWW layer (Fig. 7). Remarkably, the recovery and further analysis of *dsrAB* gene transcripts revealed the presence in the AWW layer of the sequences distantly related to that of *Desulfotignum balticum* and

halophilic *Desulfosalsimonas propionicica*. This observation let us to an assumption, that once immersed in the AWW layer, these organisms can likely withstand the high concentrations of Mg^{2+} and remain, albeit briefly, metabolically active.

Concluding remarks

The results obtained in this study portray a very stratified indigenous prokaryotic community thriving at the edge of life in the $MgCl_2$-rich DHAL *Kryos* interface under highly chaotropic conditions. The 25-cm thick *Kryos* interface layer AWW was sampled in range from 2.27 to 3.03 M of $MgCl_2$, which corresponds to salinity of 245 – 330 PSU and water activity values from 0.747 to 0.631. Despite lying beyond the established chaotropicity and prokaryotic life boundaries, the AWW layer seems inhabited by a highly specific community of prokaryotes far different from the thriving above communities. The majority of our AWW archaeal clones (85%) were affiliated to the candidate divisions MSBL1 and HC1 that branched deeply within the Euryarchaeota. These divisions were proposed recently to comprise the majority of the archaeal clones retrieved from the deep-sea Mediterranean Sea Brine Lakes (MSBL) and surficial salt-saturated anoxic lakes (van der Wielen *et al.*, 2005; Jiang *et al.*, 2007). The divisions are equivalent in genetic depth and breadth to Halobacteriales and likely represent new orders of yet-to-be-cultivated taxa (van der Wielen *et al.*, 2005). The haloarchaeal *Kryos* AWW clones together with the clones retrieved from the Lake *Discovery* formed a distinct, deeply branched cluster within Halobacteriales, thus eventually inferring the existence of new, $MgCl_2$-adapted species or genera. Similarly to archaeal community, the AWW bacterial phylotypes belonged to hitherto uncultured hyperhalophilic organisms, present exclusively in the DHALs and in highly reduced sediments of some surficial hypersaline lakes

habitats. Noteworthy, the *Kryos* microbial community, thriving below the established chaotropicity boundary for life, previously established for the Lake *Discovery*, was found be very similar, at least at the level of 16S rRNA phylogeny, to that of the other most hypersaline anoxic environments sampled worldwide. It is plausible that obligate anaerobic hyperhalophiles, adapted to thrive in salt-saturated habitats under low-A_w conditions, possess hitherto uncharacterized mechanisms to resist chaotropicity and to be metabolically active in such harsh athallasohaline habitats (e.g. exceptional levels of cellular desiccation, or unusual and/or highly kosmotropic compatible solutes; Potts, 1994; Cray *et al.*, 2013a; Wyatt *et al.*, 2014a; 2014b). The relevance of our findings encourages digging into the genetic and metabolic diversity of these $MgCl_2$-adapted hyperhalophiles. We are, therefore, conducting additional culturing and metagenomic approaches to obtain a better understanding of the functioning of the *Kryos*-interface ecosystem.

Thus, at present, we must conclude that the question of the window of tolerance of life (i.e. cellular division and/or metabolic activity) for chaotropic activity remains yet open. Compared to Lake *Discovery*, the *Kryos* lake contains slightly elevated concentrations of the kosmotropic ions Na^+ and SO_4^{2-}. These ions, via their compensating effect against extreme chaotropicity of $MgCl_2$ solutions, are likely to enable cellular activities at $MgCl_2$ concentrations which hitherto considered incompatible with life (Hallsworth *et al.*, 2007). In concordance with our previous statement, we may conclude that life in environments with extremely high concentrations of $MgCl_2$ is unlikely. Nevertheless, the simultaneous presence of kosmotropic ions in Mg-rich environments decreases their chaotropicity and thus, turns them inhabitable for diverse hyperhalophilic microbes. This assumption also has implications for hypersaline Mg-rich milieu, which are known to be located in extraterrestrial environments. However, chaotropic substances such as $MgCl_2$ can be beneficial at low temperatures (those below 10°C, and most especially sub-zero temperatures) by enhancing the flexibility of macromolecule systems, which permits cellular function and thereby reduces the

temperature minimum for cell division of psychrotolerant or psychrophilic microbes (Chin *et al.*, 2010). Ironically, therefore, the possibility remains that high concentrations of $MgCl_2$ (or other chaotropic salts) on moons or other planetary bodies, which are colder than Earth may potentially increase habitability of aqueous milieu.

Experimental procedures

Oceanographic and geophysical characterization of Kryos basin

The morphobathymetric analysis of the Mediterranean Sea at 500 m resolution (Loubriueu *et al.*, 2008) was used to locate confined depressions deeper or equal than known DHALs interfaces depths (on average 3200-3300m). The target areas were therefore investigated with the RV *Urania* hull mounted 16 transducer Benthos 3.5 KHz Chirp SBP looking at any perfectly straight line of reflection, produced by the sharp salinity : density contrast at the seawater : brine interface. Multibeam swath bathymetry was obtained by the R/V *Urania* Kongsberg-Simrad EM-302 and processed with Neptune, CARIS and GMT packages (Wessel *et al.*, 2013).

Sampling of halocline and brine in the Kryos Lake

Sampling of the *Kryos* Lake was conducted from the RV *Urania* at location (22°01'E 35°02'N – 22°02'E 34°53'N) during two oceanographic cruises in September-October 2008 and September 2009 (Fig.1b). Samples were collected using 12-litre Niskin bottles housed on a rosette (General Oceanics, Inc., Miami, FL, USA) equipped with SBE-911plus conductivity-temperature-depth (CTD) sensors (Sea-Bird Electronics, Inc., Bellevue, WA, USA). Determination of oxygen concentration at chosen depths was carried out using the Winkler method (Carpenter, 1965) with an automatic endpoint detection

burette 716 DNS Titrino (Metrohm AG, Herisau, Switzerland). Samples for determining major ion concentrations were collected in 1000 ml dark polyethylene (DPE) vials and stored at room temperature. Alternatively, 110 ml of the samples were diluted with double volume of 0.1 M of HNO_3 and stored in 500 ml DPE vials under room temperature prior the chemical analyses. Samples for determining nutrient concentrations were collected in 20 ml DPE vials, quickly frozen in liquid nitrogen and then stored at -20°C. Nutrient concentrations were determined within a few weeks of the end of each cruise using SEAL QuAAtro Microflow Analyzer (SEAL Analytical, ltd, Hampshir, UK). All running standards were prepared with Low Nutrient Seawater and calibrated against Ocean Scientific Standards (OSIL, Hampshir, UK). Sample analyses were performed at least twice using the same set of equipment. The interface was captured and fractionated as described elsewhere (Daffonchio *et al.*, 2006; Hallsworth *et al.*, 2007; Yakimov *et al.*, 2013). Briefly, 12-L Niskin bottles housed on a rosette with a CTD sensors were closed when a large increase in conductivity, indicating that the interface had been entered, was observed. This was confirmed on-board by measuring the refractive index of the top and bottom of the brine in the Niskin bottles using a hand refractometer (Atago, Tokyo, Japan). Fractions (about 0.5 - 2 l) of the captured interface were sub-sampled and preserved in sealed bottles. Redox potentials (Eh) of subsamples were measured immediately according to the procedure described by Pearson and Stanley (1979). The samples possessing the equal values of salinities were pooled for further treatments as reported below. Among all fractionated samples, the interface layers UIF, CHW and AWW, with salinities of 50-140 PSU, 140-245 PSU and 245-330 PSU, respectively, were subjected to comprehensive analysis of autochthonous microbial life. Moreover, 5 l of the *Kryos* brine was sampled for comparative purposes from the depth 3370 m.

Geochemical analyses

Dissolved cations, anions and organic acids were quantified from diluted samples using standard ion chromatographic techniques, as described below. Conductivity measurements of the samples, determined by a Conductivity meter HI 9818 (Hanna Instruments, Italy), were used to program the dilution. Na^+, K^+, Mg^{2+} and Ca^{2+} concentrations were measured using ion exchange chromatography, with a 761 Compact IC ion chromatography system (Metrohm AG, Switzerland) fitted with Metrosep C 4 column used without chemical suppression (direct conductivity and reverse polarity modality). Components were separated using a phosphoric acid (5mM) gradient, with a flow of 1 ml min^{-1}. Volatile fatty acids and sulfate concentrations were measured by ion exchange chromatography using an ICS-2000 ion chromatography system (Dionex®, UK) fitted with two AS15-HC 4 mm columns in series, and a Dionex® Anion Self-Regenerating Suppressor (ASRS®-ULTRA II 4-mm) unit in combination with a Dionex®DS6 heated conductivity cell. Components were separated using a potassium hydroxide gradient program as follows: 6.0 mmol KOH (38 min isocratic), 16.0 mmol KOH min^{-1} to 70 mmol (17 min isocratic). For chloride (Cl^-) concentrations, column was exchanged with a Ionpac AS9-SC. Chloride were separated using a sodium carbonate (Na_2CO_3) at 2 mmol and sodium bicarbonate ($NaHCO_3$) at 0.75 mmol with a flow of 1.0 ml min^{-1}.

Extraction of dissolved organic matter

Untreated brine (200 ml) was filtered through pre-combusted Whatman GF/F glass fiber filters. The pH was adjusted to 2.0 by using high purity grade formic acid (98 %). Solid-phase extraction (SPE) was followed using Agilent Bond Elut PPL SPE cartridges filled with highly functionalized styrene-divinylbenzene (SDVB) polymer that has been modified with a proprietary non-polar surface. The SPE cartridge was activated using methanol (Sigma-Aldrich Chromasolv LC-MS grade methanol), washed with acidified (pH 2.0) high purity water (Sigma-Aldrich Chromasolv LC-MS grade water). Then, the acidified sample was gravity-fed through the SPE cartridge. The cartridge was washed again with acidified pure water to replace the last remaining inorganic ions from the

SPE cartridge. After washing, the cartridge was dried under high purity grade nitrogen gas and eluted with methanol.

Ultrahigh resolution mass spectrometry

Ultrahigh-resolution mass spectra were acquired on a Bruker (Bremen, Germany) APEX 12 Qe Fourier transform ion cyclotron resonance mass spectrometer equipped with a 12 T superconducting magnet and a APOLLO II electrospray source. The SPE methanol eluate was diluted 1:20 into methanol and introduced into the micro electrospray source at a flow rate of 120 mL/h with a nebulizer gas pressure of 20 psi (138 kPa) and a drying gas pressure of 15 psi (103 kPa) at 250°C through an Agilent sprayer. Spectra were externally calibrated on clusters of arginine (5 mg l^{-1} in methanol) and systematically internally calibrated with appropriate reference mass list reaching accuracy values lower than 100 ppb in routine day-to-day measurements. Data acquisition was performed using DataAnalysis associated software (Bruker Daltonics, version 4.0). The possible elemental formulas were calculated from the exported masses list for each peak in batch mode by a software tool written in-house (Netcalc). The generated formulas were validated by setting sensible chemical constraints (N rule, double bond equivalent non-negative integers, O/C ratio ≤1, H/C ratio ≤2+2/n (where n is the number of carbon). Van Krevelen diagrams (H/C vs O/C) and (H/C vs m/z) diagrams were used to visualize these datasets.

Quantitation of water activity and chaotropic activity

Besides the natural *Kryos* brine, an artificial analogue brine was also used for water activity and chaotropicity determination. This synthetic, analogue 'Lake *Kryos*' brine was made up by dissolving following salts: $MgCl_2$ (4.1841 M), $MgSO_4$ (0.2183 M), Na_2SO_4 (62 mM) K_2SO_4 (42.2 mM), $CaCl_2$ (1 mM), $(NH_4)_2SO_4$ (0.4 mM) which was stored for one week at 14.3°C prior to water-activity determinations.

Water activities were determined over a range of concentrations at 14.3°C using a Novasina IC II water activity machine fitted with an alcohol-resistant humidity sensor and eVALC alcohol filter (Novasina, Pfäffikon, Switzerland), as described previously (Hallsworth and Nomura, 1999). This brine was super-saturated as a fine, powdery precipitate could be seen by eye. For quantification of chaotropic activity, agar gel-points were determined over a range of salt or brine concentrations (see Hallsworth *et al.*, 2003a; 2007) using a Cecil E2501 spectrophotometer fitted with a thermoelectrically controlled heating block (Milton Technical Centre, Cambridge, England) as described previously (Cray *et al.*, 2013a).

CARD-FISH analysis

CARD-FISH samples (50 ml) were collected from overalying seawater, the interface layers UIF, CHW, AWW and the *Kryos* brine. Samples were fixed with 2% formaldehyde (v/v, final concentration) at room temperature for 1 hour and stored at -20°C in the dark until laboratory analysis. Subsamples (from 1 to 10 ml, according to cell concentrations) were filtered through polycarbonate membranes (Ø25 mm, 0.22 µm pore size, NTG). Cells were permeabilized with lysozyme (10 mg ml^{-1}, 1 h) and achromopeptidase (5 mg ml^{-1}, 30 min) at 37°C. Intracellular peroxidase was inhibited by treatment with HCl (0.01 mmol l^{-1}) at room temperature for 20 min. We used the following horseradish peroxidase labeled probes: EUB338 I-III, ARCH915, CREN537, EURY806, KB1, and Delta-DHAL. Detailed information about the probes shown in Table S1. The nonspecific probe NON338 did not detect any cells. The filters sections were counter-stained with DAPI (2 mg ml^{-1}) in a 4:1 ratio of Citifluor (Citifluor Ltd, Leicester, UK) and Vectashield (Linaris GmbH, Wertheim- Bettingen, Germany). At least 200 DAPI cells, in a minimum of 10 fields, were counted in the AXIOPLAN 2 Imaging microscope (Zeiss). Negative control counts were performed with HRP-Non338 probe, always amounting to < 1% of DAPIstained cells.

Nucleic acid purification and cDNA synthesis

For DNA/RNA extraction, 2-5 l of the fractionated interface and brine samples were filtered through sterile Sterivex capsules (0.2µm pore size, Millipore) using a peristaltic pump. After filtration, filters were treated with 400µl of TE buffer (pH 8.0) containing lysozyme (5 mg ml^{-1}), vortexed for 5 sec and incubated 10 min at room temperature. 1600µl of lysis buffer QRL1 (containing β-mercaptoethanol) were added and filters were than stored at -20°C until processing. Total DNA and RNA were extracted using Qiagen RNA/DNA Mini Kit (Qiagen, Milan, Italy). The extraction was carried out according to the manufacturer's instructions. DNA and RNA samples were examined by agarose gel electrophoresis and concentrations were determined using the NanoDrop ND-1000 Spectrophotometer (Wilmington, DE, USA). RNA-containing extracts were purified from DNA by Turbo DNA-free kit (Ambion, Austin, TX, USA). Each RNA sample was immediately converted into cDNA with SuperScript II Reverse Transcriptase (Invitrogen, Carlsbad, CA, USA) and hexa-random primers according to the manufacturer instructions.

PCR-amplification, gene cloning and sequencing

Bacterial 16S *rRNA*, archaeal 16S *rRNA* and key genes involved in sulphur respiration (*dsr*AB) and methanogenesis (*mcr*A), were amplified by PCR using primers listed in the Table S1. All reactions were carried out in a MasterCycler 5331 Gradient PCR (Eppendorf, Hamburg, Germany). The conditions for PCR and cloning were performed as described elsewhere (La Cono *et al.*, 2011, Yakimov *et al.*, 2013). Positive clones from each library were randomly selected by PCR amplification. The PCR products were further purified and sequenced at Macrogen (Amsterdam, Netherlands).

Phylogenetic trees

Pintail software (Ashelford *et al.*, 2005) was used to check sequences for possible chimeric origin. 16S rRNA gene amplified sequences and close relatives identified with BLAST (Altschul *et al.*, 1997) were aligned using the SILVA alignment tool (Pruesse *et al.*, 2007) and manually checked with ARB (Ludwig *et al.*, 2004). MEGA 5 (Tamura *et al.*, 2007) was used to align functional genes nucleotides sequences. After alignment, the neighbor-joining algorithm of ARB and MEGA 5 program packages were used to generate the phylogenetic trees based on distance analysis for 16S rRNA and functional genes, respectively. The robustness of inferred topologies was tested by bootstrap re-sampling using the same distance model (1,000 replicates). Significant difference of the microbial assemblages derived from different samples depths was detected via the *P*-test significance and principal coordinates analysis (PCA) using UniFrac program (http://bmf2.colorado.edu/fastunifrac (Hamandy *et al.,* 2009; Lozupone *et al.,* 2007) for comparison of the microbial communities using phylogenetic information.

Nucleotide sequence accession numbers

The nucleotide sequences produced in the present study have been deposited in the DDBJ/EMBL/GenBank databases under accession numbers: KJ922395 to KJ922487 for the bacterial and archaeal 16S rRNA gene sequences, KJ922632 to KJ922638 for the archaeal *mcr*A gene sequence, KJ922623 to KJ922631 for the bacterial *dsr*A gene sequences.

Acknowledgements

This work was performed with the financial support of CNR in frames of the EU FP7 Projects MAMBA (KBBE-2009-2B-226977) and MicroB3 (OCEAN 2011-2-287589). JAC was supported by funding received from the Department of Agriculture and Rural Development (Northern Ireland). We thank the Master, crew of RV *Urania* and all participants to the cruises for their valuable professionalism and

support during the cruises. A. Modica, M. Catalfamo are indebted for geochemical analyses. The discoveries were possible only because of good topographic data made available by other Institutions, and we thank Dr. Benoit Loubrieu of IFREMER for providing the 500m-resolution DTM data.

References

Altschul, S.F., Madden, T.L., Schäffer, A.A., Zhang, J., Zhang, Z., Miller,W., *et al.* (1997) Gapped BLAST and PSI-BLAST: a new generation of protein database search programs. *Nucleic Acids Res* **25**: 3389–3402.

Ashelford, K.E., Chuzhanova, N.A., Fry, J.C., Jones, A.J., and Weightman, A.J. (2005) At least 1 in 20 16S rRNA sequence records currently held in public repositories is estimated to contain substantial anomalies. *Appl Environ Microbiol* **71**: 7724–7736.

Baati, H., Guermazi, S., Gharsallah, N., Sghir, A. and Ammar, E. (2010) Novel prokaryotic diversity in sediments of Tunisian multipond solar saltern. *Res Microbiol* **161:** 573-582.

Bell, A.N.W., Magill, E., Hallsworth, J.E., and Timson, D.T. (2013) Effects of alcohols and compatible solutes on the activity of ß-galactosidase. *Appl Biochem Biotech* **169**: 786–796.

Bhaganna, P., Volkers, R.J.M., Bell, A.N.W., Kluge, K. Timson, D.J., McGrath, J.W., Ruijssenaarsm H.J., and Hallsworth, J.E, (2010) Hydrophobic substances induce water stress in microbial cells. *Microb Biotechnol* **3**: 701–716.

Borin, S., Brusetti, L., Mapelli, F., D'Auria, G., Brusa, T., Marzorati, M., *et al.* (2009) Sulfur cycling and methanogenesis primarily drive microbial colonization of the highly sulfidic Urania deep hypersaline basin. *Proc Natl Acad Sci U S A* **106:** 9151-9156.

Borrel, G., O'Toole, P.W., Harris, H.M., Peyret, P., Brugère, J.F. and Gribaldo, S. (2013) Phylogenomic data support a seventh order of methylotrophic methanogens and provide insights into the evolution of methanogenesis. *Genome Biol Evol* **5:** 1769-1780.

Camerlenghi, A. (1990) Anoxic basins of the eastern Mediterranean: geological framework. *Mar Chem* **31:** 1-19.

Camerlenghi, A., and McCoy, F.W. (1990) Physiography and structure of Bacino Bannock (Eastern Mediterranean). *Geo-Mar* Lett **31:** 21-33.

Carpenter, A.B. (1978) Origin and chemical evolution of brines in sedimentary basins. *Oklahoma Geol Surv Circ* **79:** 60-77.

Chamot-Rooke, N. Rabaute, A., and Kreemer, C. (2005) Western Mediterranean Ridge mud belt correlates with active shear strain at the prism-backstop geological contact. *Geology* **33:** 861-864.

Chin, J.P., Megaw, J., Magill, C.L., Nowotarski, K., Williams, J.P., Bhaganna, P., Linton, M., Patterson, M.F., Underwood, G.J.C, Mswaka, A.Y., and Hallsworth, J.E. (2010) Solutes determine the temperature windows for microbial survival and growth. *Proc Natl Acad Sci* **107**: 7835–7840.

Cita, M.B. (1991) Anoxic basins of the eastern Mediterranean: An overview. *Paleoceanography* **6:** 133-141.

Cita M.B. (2006) Exhumation of Messinian evaporites in the deep-sea and creation of deep anoxic brine-filled collapsed basins. *Sediment Geol* **188-189:** 357-378

Cray, J.A., Russell, J.T., Timson, D.J., Singhal, R.S., and Hallsworth, J.E. (2013a) An universal measure of chaotropicity and kosmotropicity. *Environ Microbiol* **15**: 287–296.

Cray, J.A., Bell, A.N.W., Bhaganna, P., Mswaka, A.Y., Timson, D.J., and Hallsworth, J.E. (2013b) The biology of habitat dominance; can microbes behave as weeds? *Microb Biotechnol* **6**: 453–492.

Daffonchio, D., Borin, S., Brusa, T., Brusetti, L., van der Wielen, P.W., Bolhuis, H., *et al.* (2006). Stratified prokaryote network in the oxic-anoxic transition of a deep-sea halocline. *Nature* **440:** 203-207.

De Lange, G.J. and Ten Haven H.L. (1983) Recent sapropel formation in the eastern Mediterranean. *Nature* **305:** 797-798.

De Lange, G.J., Middleburg, J.J., van der Weijden, K.H., Luther III, G.W., Hydes, D.J., Woittiez, J.R.W., *et al.* (1990) Composition of anoxic hypersaline brines in the Tyro and Bannock Basins, Eastern Mediterranean. *Mar Chem* **31:** 63-88.

Demergasso, C., Escudero, L., Casamayor, E.O., Chong, G., Balague, V. and Pedros-Alio, C. (2008) Novelty and spatio-temporal heterogeneity in the bacterial diversity of hypersaline Lake Tebenquiche (Salar de Atacama). *Extremophiles* 12: 491-504.

Dridi, B., Fradeau, M.-L., Ollivier, B., Raoult, D., and Drancourt, M. (2012) *Methanomassiliicoccus luminyensis* gen. nov., sp. nov., a methanogenic archaeon isolated from human faeces. *Int J Syst Evol Microbiol* **62:** 1902-1907.

Doroshenko, E.A., Zenova, G.M., Zvyagintsev, D.G., and Sudnitsyn, I.I. (2005) Spore germination and mycelial growth of streptomycetes at different humidity levels. *Mikrobiologiia* **74**: 690–694.

Doroshenko, E.A., Zenova, G.M., Sudnicin, I.I., and Zvyagintsev, D.G. (2006) Influence of humidity on soil mycelial bacteria. *Vestn Mosk U Poch* **1**: 45–48.

Duda, V.I., Danilevich, V.N., Suzina, N.E., Shorokhova, A.P., Dmitriev, V.V., Mokhova, O.N., and Akimov, V.N. (2004) Changes in the fine structure of microbial cells induced by chaotropic salts. *Mikrobiologiya* **73**: 341–349.

Feike, J., K. Jürgens, J. T. Hollibaugh, S. Krüger, G. Jost and M. Labrenz (2012). Measuring unbiased metatranscriptomics in suboxic waters of the central Baltic Sea using a new in situ fixation system. *ISME J* **6:** 461-470.

Grant, W.D. (2004) Life at low water activity. *Philos Trans R Soc Lond B Biol Sci* **359**: 1249–1266.

Grolas, A., Robert, C., Gimenez, G., Drancourt, M. and Raoult D. (2012) Complete genome sequence of *Methanomassiliicoccus luminyensis*, the largest genome of a human-associated Archaea species. *J Bacteriol* **194:** 4745.

Hallsworth, J.E., and Nomura, N. (1999) A simple method to determine the water activity of ethanol-containing samples. *Biotechnol Bioeng* **62:** 242–245.

Hallsworth, J.E., Heim, S. and Timmis, K.N. (2003a) Chaotropic solutes cause water stress in *Pseudomonas putida*. *Environ Microbiol* **5:** 1270–1280.

Hallsworth, J.E., Prior, B.A., Nomura, Y., Iwahara, M., and Timmis, K.N. (2003b) Compatible solutes protect against chaotrope (ethanol)-induced, nonosmotic water stress. *Appl Environ Microbiol* **69:** 7032–7034.

Hallsworth, J.E., Yakimov, M.M., Golyshin, P.N., Gillion, J.L., D'Auria, G., de Lima Alves, F., *et al.* (2007) Limits of life in MgCl2-containing environments: chaotropicity defines the window. *Environ Microbiol* **9:** 801-813.

Hamady M., Lozupone C.A. and Knight R., (2009) Fast UniFrac: facilitating high-throughput phylogenetic analyses of microbial communities including analysis of pyrosequencing and PhyloChip data. *The ISME Journal* (2010) **4:** 17–27.

Harrison, J.P., Gheeraert, N., Tsigelnitskiy, D., and Cockell, C.S. (2013) The limits for life under multiple extremes. *Trends Microbiol* 21: 204–212.

Hertkorn, N., Benner, R., Schmitt-Kopplin, Ph., Kaiser, K., Kettrup, A., Hedges, I.J. (2006) Characterization of a major refractory component of marine organic matter, *Geochimica Cosmochimica Acta*, **70:** 2990-3010.

Jiang, H., Dong, H., Yu, B., Liu, X., Li, Y., Ji, S., *et al.* (2007) Microbial response to salinity change in Lake Chaka, a hypersaline lake on Tibetan plateau. *Environ Microbiol* **9:** 2603-2621.

Kurapova, A.I., Zenova, G.M., Sudnitsun, I.I., Kizilova, A.K., Manucharova, N.A., Norovsuren, Zh., and Zvyagintsev, D.G. (2012) Thermotolerant and thermophilic actinomycetes from soils of Mongolia desert steppe zone. *Microbiology* **81**: 98–108.

La Cono V, Smedile F, Bortoluzzi G, Arcadi, E., Maimone, G., Messina, E. et al. (2011) Unveiling microbial life in new deep-sea hypersaline Lake Thetis. Part I: Prokaryotes and environmental settings. *Environm Microbiol* **13**: 2250-2268.

Lievens, B., Hallsworth J.E., Belgacem, Z.B., Pozo, M.I., Stevenson, A., Willems, K.A., and H. Jacquemyn (2014) Microbiology of sugar-rich environments: diversity, ecology, and system constraints. *Environmental Microbiology Reports* (in press).

Loubrieu B., Mascle J. Benkhelil, J., Bernè, S., Chamot-Rooke, N., Deverchère, J. *et al.* (2008) Morpho-bathymetry of the Mediterranean Sea, CIESM/Ifremer Medimap Group, CIESM edition.

Lozupone, C.A., Hamady, M., Kelley, S.T. and Knight, R. (2007) Quantitative and qualitative beta diversity measures lead to different insights into factors that structure microbial communities. *Appl Environ Microbiol* **73**: 1576–1585.

Ludwig, W., Strunk, O., Westram, R., Richter, L., Meier, H., Yadhukumar, B., *et al.* (2004) ARB: a software environment for sequence data. *Nucleic Acids Res* **32**: 1363–1371.

Makhdoumi-Kakhki, A., Amoozegar, M.A., Kazemi, B., Pasic, L. and Ventosa, A. (2012) Prokaryotic diversity in Aran-Bidgol Salt Lake, the largest hypersaline Playa in Iran. *Microbes Environ* **27:** 87-93.

Marion, G.M., Fritsen, C.H., Eicken, H., and Payne, M.C. (2003) The search for life on Europa: limiting environmental factors, potential habitats, and earth analogues. *Astrobiol* **3:** 785–811.

McCaffrey, M.A., Lazar, B. and Holland, H.D., (1987) The evaporation path of seawater and the coprecipitation of Br^- and K^+ with halite. *J Sediment Petrol* **57:** 928-937.

MEDRIFF Consortium (1995) Three brine lakes discovered in the seafloor of the eastern Mediterranean. *EOS Trans AGU* **76:** 313.

Oren, A. (1983) *Halobacterium sodomense* sp. nov., a Dead Sea *Halobacterium* with an extremely high magnesium requirement. *Int J Syst Bacteriol* **33:** 381–386.

Oren, A. (1999) Bioenergetic aspects of halophilism. *Microbiol Mol Biol Rev* **63**: 334–348.

Oren, A. (2010) The dying Dead Sea: the microbiology of an increasingly extreme environment. *Lakes Reser: Res Manag* **15**: 215–222.

Pearson, T.H., and Stanley, S.O. (1979) Comparative measurements of the redox potential of marine sediments as a rapid means of assessing the effect of organic pollution. *Mar Biol* **53:** 371–379.

Pitt, J.I. and Christian, J.H.B. (1968) Water relations of xerophilic fungi isolated from prunes. *Appl Environ Microbiol* **16:** 1853–1858.

Pitt, J.I. (1975) Xerophilic fungi and the spoilage of foods of plant origin. In *Water Relations of Foods*. Duckworth, R.B. (ed.). London, United Kingdom: Academic Press, pp. 273–307.

Potts M (1994) Desiccation tolerance of prokaryotes. *Microbiol Rev* **58**:755–805.

Pruesse, E., Quast, C., Knittel, K., Fuchs, B.M., Ludwig, W., Peplies, J., *et al.* (2007) SILVA: a comprehensive online resource for quality checked and aligned ribosomal RNA sequence data compatible with ARB. *Nucleic Acids Res* **35**: 7188–7196.

Raup, O.B. (1970) Brine mixing: An additional mechanism for the formation of evaporate brines. *Bulletin of the American Association of Petroleum Geologists* **54**: 2246–2259.

Tamura, K., Peterson, D., Peterson, N., Stecher, G., Nei, M., and Kumar, S. (2011) MEGA5: molecular evolutionary genetics analysis using maximum likelihood, evolutionary distance, and maximum parsimony methods. *Mol Biol Evol* **28**: 2731–2739.

Schmitt-Kopplin, Ph., Gelencser, A., Dabek-Zlotorzynskaya, E., Kiss, G., Hertkorn, N., Harir, *et al.* (2010a) Analysis of the unresolved organic fraction in atmospheric aerosols with ultrahigh-resolution mass spectrometry and nuclear magnetic resonance spectroscopy: organosulfates as photochemical smog constituents. *Anal Chem* **82:** 8017-8016.

Schmitt-Kopplin, Ph., Gabelica, Z., Gougeon, R.D., Fekete, A., Kanawati, B., Harir, M. *et al.* (2010b) High molecular diversity of extraterrestrial organic matter in Murchison meteorite revealed 40 years after its fall. *PNAS* **107:** 2763-2768.

Stevenson, A. and Hallsworth, J.E. (2014) Water and temperature relations of soil Actinobacteria. Revised for *Environmental Microbiology Reports*.

Stevenson, A., Burkhardt, J., Cockell, C.S., Cray, J.A., Fox-Powell, M., Kee, T.P., *et al.* (2014) Multiplication of microbes below 0.690 water activity: implications for terrestrial and extraterrestrial life. Under revision for *Environmental Microbiology*.

van der Wielen, P.W., H. Bolhuis, J.J., Borin, S., Daffonchio, D., Corselli, C., Giuliano, L., *et al.* (2005) The enigma of prokaryotic life in deep hypersaline anoxic basins. *Science* **307:** 121-123.

Wallmann, K.J., Suess, E., Westbrook, G.H., Winckler, G., Cita, M.B., and the Medriff consortium (1997) Salty brines on the Mediterranean sea floor. *Nature* **387:** 31-32.

Wallmann, K., Aghib, F.S., Castradori, D., Cita, M.B., Suess, E., Greinert, J., and Rickert, D. (2002) Sedimentation and formation of secondary minerals in the hypersaline Discovery Basin, eastern Mediterranean. *Mar Geol* **186:** 9–28.

Wessel, P., Smith, W.H.F., Scharroo, R., Luis, J.F. and Wobbe F. (2013) Generic mapping tools: improved version released, *EOS Trans AGU* **94:** 409-410.

Williams, J.P., and Hallsworth, J.E. (2009) Limits of life in hostile environments; no limits to biosphere function? *Environ Microbiol* **11**: 3292–3308.

Winston, P.W. and Bates, P.S. (1960) Saturated salt solutions for the control of humidity in biological research. *Ecology* **41**: 232–237.

Yakimov, M.M., La Cono, V., Denaro, R., D'Auria, G., Decembrini, F., Timmis, K.N., *et al.* (2007a) Primary producing prokaryotic communities of brine, interface and seawater above the halocline of deep anoxic lake L'Atalante, Eastern Mediterranean Sea. *Int Soc Microb Ecol* J **1:** 743-755.

Wyatt, T.T., Golovina, E.A., van Leeuwen, M.R., Hallsworth, J.E., Wösten, H.A.B. and J. Dijksterhuis (2014a) Decreases in bulk water and mannitol and accumulation of trehalose and trehalose-based oligosaccharides define a two-stage maturation process towards extreme stress-resistance in ascospores of *Neosartorya fischeri* (*Aspergillus fischeri*). *Environmental Microbiology* In press (doi: 10.1111/1462-2920.12557).

Wyatt, T.T., van Leeuwen, M.R., Gerwig, G.J., Golovina, E.A., Hoekstra, F.A., Kuenstner, E.J., *et al.* (2014b) Functionality and prevalence of trehalose-based oligosaccharides as novel compatible solutes in ascospores of *Neosartorya fischeri* (*Aspergillus fischeri*) and other fungi. *Environmental Microbiology* In press (doi: 10.1111/1462-2920.12558).

Yakimov, M.M., Giuliano, L., Cappello, S., Denaro, R., and Golyshin, P.N. (2007b) Microbial Community of a Hydrothermal Mud Vent Underneath the Deep-Sea Anoxic Brine Lake Urania (Eastern Mediterranean). *Orig Life Evol Biosph* **37:** 177-188.

Yakimov, M.M., La Cono, V., Slepak, V.Z., La Spada, G., Arcadi, E., Messina, E., *et al.* (2013) Microbial life in the Lake *Medee*, the largest deep-sea salt-saturated formation. *Sci Report* **3:** 3554

Zvyagintsev, D.G., Zenova, G.M., Doroshenko, E.A., Gryadunova, A.A., Gracheva, T.A., and Sudnitsyn, I.I. (2007) Actinomycete growth in conditions of low moisture. *Izv Akad Nauk Ser Biol* **34**: 242–247.

Zvyagintsev, D.G., Zenova, G.M., Sudnitsyn, I.I., Gracheva, T.A., Napol'skaya, K.R., and Belousova, M.A. (2009) Dynamics of spore germination and mycelial growth of streptomycetes under low humidity conditions. *Microbiology* **78**: 440–444.

Zvyagintsev, D.G., Zenova, G.M., Sudnitsyn, I.I., Gracheva, T.A., Lapygina, E.E., Napol'skaya, K.R., and Sydnitsyna, A.E. (2012) Development of actinomycetes in brown semidesert soil under low water pressure. *Eurasian Soil Sci* **45**: 717–725.

Table 1. Chemical composition of the three saltiest DHALs on Earth.

	DISCOVERY*	KRYOS	L'ATALANTE
Salinity, g kg^{-1}	**510**	**471**	**352**
Distance of lake surfac bsl, m	3580	3337	3428
Brine depth, m	55	160	80
Brine temperature, °C	16.1	14.5	14.3
Density, kg l^{-1}	1.33	1.31	1.23
Na, g kg^{-1}	1.93	2.84	107
Cl, g kg^{-1}	360	321	188
Mg, g kg^{-1}	125	107	16
K, g kg^{-1}	3.5	3.3	14.4
Ca, g kg^{-1}	0.04	0.04	0.3
SO_4, g kg^{-1}	10.6	31	32
Br, g kg^{-1}	8.81	5.60	0.49
$\sum O_2$, g kg^{-1}	0.18	0.66	1.54
Li, mg kg^{-1}	4.9	3.7	0.5
H_2S, mg kg^{-1}	29	41	96
NH_4, mg kg^{-1}	11	16	52
B, mg kg^{-1}	283	362	13.2
PO_4, mg kg^{-1}	5.6	6.8	1.2

These data were partially taken from Wallmann *et al.* 1997, 2002.

Table 2. Chemical compositions of the most anhydrous (A_w < 0.700) athalassohaline lakes on Earth and primary (LSPB) and secondary (SB) brines. All concentrations are in mM (kg H_2O)$^{-1}$ unless otherwise stated.

	LSPB[a]	SB[b]	DEAD SEA[c]	DON JUAN POND[c]	DISCOVERY	KRYOS
Major ions, mM kg^{-1}						
Na	166	99	1835	112	84	125
Mg	5410	5410	1944	110	5150	4379
K	71	112	212	8	90	80
Ca	1	3	459	5830	1	1
SO_4	173	122	6	<1	110	320
Cl	10100	10926	6824	12192	10150	9043
Parameters						
pH	~5.6[a]	~5.6[a]	7.7	~5.4[a]	~4.5[a]	~5.4[a]
Water activity, A_w	**0.420**	**0.380**	0.690	**0.411**	**0.382**	**0.399**
Salinity, g kg^{-1}	513	515	359	670	510	471
Density, kg L^{-1}	1.33	1.33	1.22	1.39	1.33	1.32

[a] As it described elsewhere (Wallmann *et al.*, 1997, 2002), the late stage primary brine (LSPB) was produced by evaporation of seawater and precipitation of anhydrite ($CaSO_4$), halite (NaCl), kieserite ($MgSO_4 \cdot H_2O$) and carnallite ($KMgCl_3 \cdot 6H_2O$). The evaporation was performed at atmospheric pressure and 30°C and continued until only 5g of the initial 1 kg H_2O remained in solution.

[b] Secondary brine (SB) produced by equilibrating of calcite-saturated seawater with the evaporite minerals bischofite ($MgCl_2 \cdot 6H_2O$), kainite ($KMg(SO_4)Cl \cdot 3H_2O$), halite, and gypsum ($CaSO_4 \cdot 2H_2O$) at 14°C and 1 atm (Wallmann *et al.*, 2002).

[c]Composition of the Dead Sea (Israel) and the Don Juan Pond (Antarctica) were taken from Marion *et al.* 2003. Water activity values below the window of cellular life (A_w <0.605) are highlighted in bold.

Table 3. Abundance of general and specific phylogenetic groups within *Bacteria* and *Archaea* in the *Kryos* interface layers and overlaying seawater.

The total cell numbers are given as 10^5 cells ml^{-1} unless otherwise stated. Cells were collected from the indicated layers and hybridized with the specific CARD-FISH probes (Yakimov *et al.*, 2013).

Interface layer[a], (Mg^{2+}, M / salinity, PSU)	DAPI	EUB338 I-III	KB1	Delta-DHAL	ARCH915	CREN537	EURY806
SW[b]	0.16±0.02	0.12±0.02	0	0	0.02±0.008	0.02±0.004	0
UIF (0.16/52)	0.93±0.10	0.32±0.08	0	0	0.17±0.05	0.16±0.02	0.02±0.01
CHW (1.55/195)	5.57±0.45	2.97±0.56	0.17±0.03	0.14±0.04	0.81±0.77	0.05±0.01	0.22±0.01
AWW1 (3.03/327)	4.60±0.43	2.45±0.21	0.69±0.12	0.14±0.03	0.43±0.07	0	0
AWW2 (3.41/370)	2.47±0.11	1.53±0.07	1.22±0.11	0.13±0.01	0.47±0.05	0	0

[a] See Figure 2 for exact positioning of sampling points within three layers of the *Kryos* interface.

[b] These data correspond to the seawater column sampled from the depth of 2850 m twenty nautical miles NE from the Lake *Kryos* during the same cruise as it described elsewhere (La Cono *et al.* 2011).

Figure legends

Figure 1. Location of currently known DHALs in the Eastern Mediterranean Sea (a) and the detailed swath bathymetry at the *Kryos* Lake area (b).

The map to the left was constructed using the Ocean Data View software (Schlitzer *et al.*, 2010). On the right, the shape of the anoxic lake and small polar satellite pools are colored in blue starting from the seawater : brine lake interface (3337 m depth). The sampling sites are highlighted by asterisks.

Figure 2. Physicochemical activities of $MgCl_2$ solutions, the Lake *Kryos* brine and a synthetic *Kryos*-brine analogue: (a) water-activity reduction over a range of $MgCl_2$ concentrations at 14.3°C (for comparative purposes all values are expressed according to their $MgCl_2$ content) and the upper dotted line indicates the lower boundary of the previously established chaotropicity limit of life (CHW, equivalent to 2.3 M $MgCl_2$; Hallsworth *et al.*, 2007) and the lower dotted line denotes the established water-activity limit for xerophilic fungi (AWW; Pitt and Christian, 1968); and (b) agar gel-point depression (a measure of chaotropic activity; Cray *et al.*, 2013a).

The solid lines with arrows indicate the water-activity values corresponding to the AWW layer ($MgCl_2$ 2.27 - 3.03 M).

Figure 3. Depth profiles of geochemical markers through the Lake *Kryos* and the established boundary for chaotropicity and xerophilic cellular life occurred in the *Kryos* gradient.

As far as all conventional on-line CTD sensors were not functional in $MgCl_2$-rich ambience, chemical analysis of fractionated interface samples were performed in the in-land laboratory. The brine was collected at the depths of 3340 and 3370 m bsl. The layers of interface collected for the molecular

analyses are highlighted in green, blue and red. Following the A_w calculations (Fig. 2a), the boundary for chaotropicity (A_w 0.790) and xerophilic cellular life (A_w 0.605) occurred in the *Kryos* gradient are shown. Abbreviations used: AWW, the interface layer corresponding to lower boundary of estimated xerophilic cellular life; BB, body brine; CHW, the interface layer corresponding to lower boundary of chaotropicity life; UIF, upper interface. Data points are mean ± standard error (n=3).

Figure 4. Ultrahigh resolution mass spectrometry of the *Kryos* brine DOM showing hundreds of low molecular weight organic compounds (a) with m/z <500 amu. The van Krevelen diagrams (b, c) illustrate the high proportion of largely saturated structures and the remarkable extent of oxygenation of the CHNO and poly-sulfur compounds (d). The blue line refers to any fully saturated open chain aliphatic (poly)carboxylic acid, (comparable to polymaleic acid or polyacrylic acid as model structures) and the red line to the compositional range of CRAM molecules as described in Hertkorn *et al.* (2006).

Figure 5. Overview on prokaryotic diversity, stratification (a) and relative abundance (b) of phylogenetic groups recovered from the different compartments of Lake *Kryos.*

(a) Stratification and relative abundance of each phylogenetic group found in different layers of the Lake *Kryos* is shown as number of cloned and analysed sequences related to the indicated group. The clones recovered from the *Kryos* brine, the upper interface (UIF), the layer of chaotropicity (CHW) and the water activity (AWW) windows are shown in black, green, blue and red, respectively. Scale bar corresponds to 10% estimated difference in nucleotide sequence positions.
(b) Extent of recovery of 16S crDNA AWW clone sequences in overlaying layers UIF and CHW. Scale white bar corresponds to 20% of all cloned sequences analyzed separately in UIF, CHW and AWW clone libraries. Exact percentages of clones corresponding to each indicated phylogenetic group are given for clarity.

Abbreviations of candidate division used: BRC1, Bacterial Rice Cluster; DP, Deltaproteobacteria; HA, haloarchaea; HC1, Halophilic Cluster 1; KB1, Kebrit Deep Bacteria 1; MH, *Methanohalophilus*; MSBLx, Mediterranean Sea Brine Lakes; OM27, Ocean Margins 27; SA1, Shaban Deep Archaea 1; SARx, Sargasso Sea Clusters.

Figure 6. Phylogenetic analyses of clone sequences of Archaea and *mcr*A gene transcripts recovered from the AWW interface layer.

The 16S rRNA phylogenetic analysis indicates the relationship between AWW archaeal clone sequences and related sequences recovered from the CHW interface layer, the *Kryos* brine and other DHALs and surficial hypersaline lakes. The analysis of sequences derived from mRNA coding for methyl co-M reductase (*mcr*A) indicates that methanogens similar to both the lake *Discovery* organisms and *Methanohalophilus halophilus* are active in the AWW layer. The white and solid cycles at the nodes indicate the percentages of recovery in 1,000 bootstrap resamplings of < 75% and ≥75%, respectively. Only relevant bootstrap values of ≥70% are shown. Scale bar corresponds to 5% estimated difference in nucleotide sequence positions. Trees were respectively rooted with *Desulfotignum balticum* 16S rRNA (AF233370) and *Methanobrevibacter arboriphilus* DSM 1125 *mcr*A (AF414035) gene sequences.

Figure 7. Phylogenetic analysis of bacterial clone sequences and *dsr*AB gene transcripts recovered from the AWW interface layer.

The phylogenetic analysis indicates the relationship between AWW bacterial clone sequences and related sequences recovered from the CHW interface layer, the *Kryos* brine and other DHALs and surficial hypersaline lakes. It also demonstrates that a taxonomic (16S rRNA) and a functional (*dsr*AB) marker give largely congruent phylogenies and the main taxa identified were

Desulfobacteraceae and *Desulfohalobiaceae*. The white and solid cycles at the nodes indicate the percentages of recovery in 1,000 bootstrap resamplings of < 75% and ≥75%, respectively. Only relevant bootstrap values of ≥70% are shown. Scale bar corresponds to 5% estimated difference in nucleotide sequence positions. Trees were respectively rooted with *Halorhabdus tiamatea* 16S rRNA (NR_113213) and *Thermodesulforhabdus norvegica dsr*AB (AF334597) gene sequences.

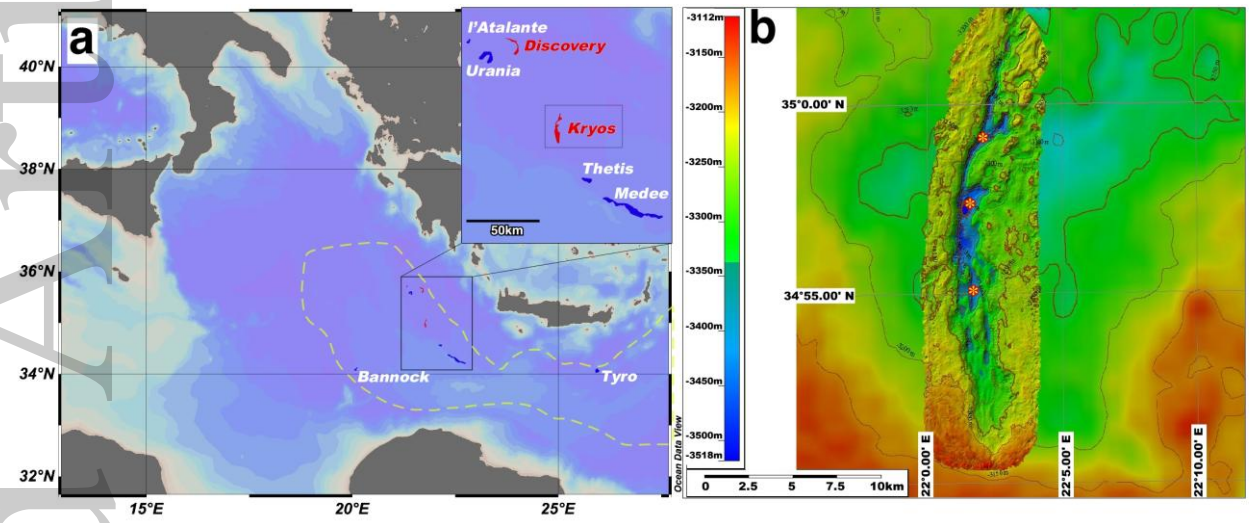

emi_12587_f1

1

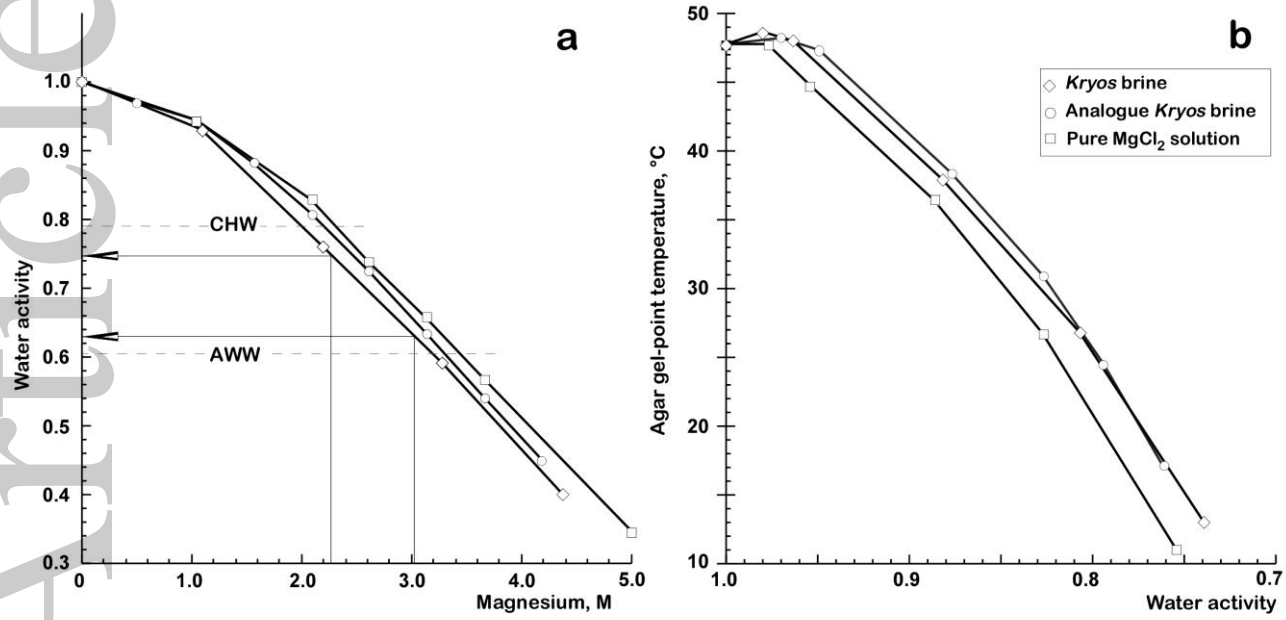

2

3 emi_12587_f2

4

1

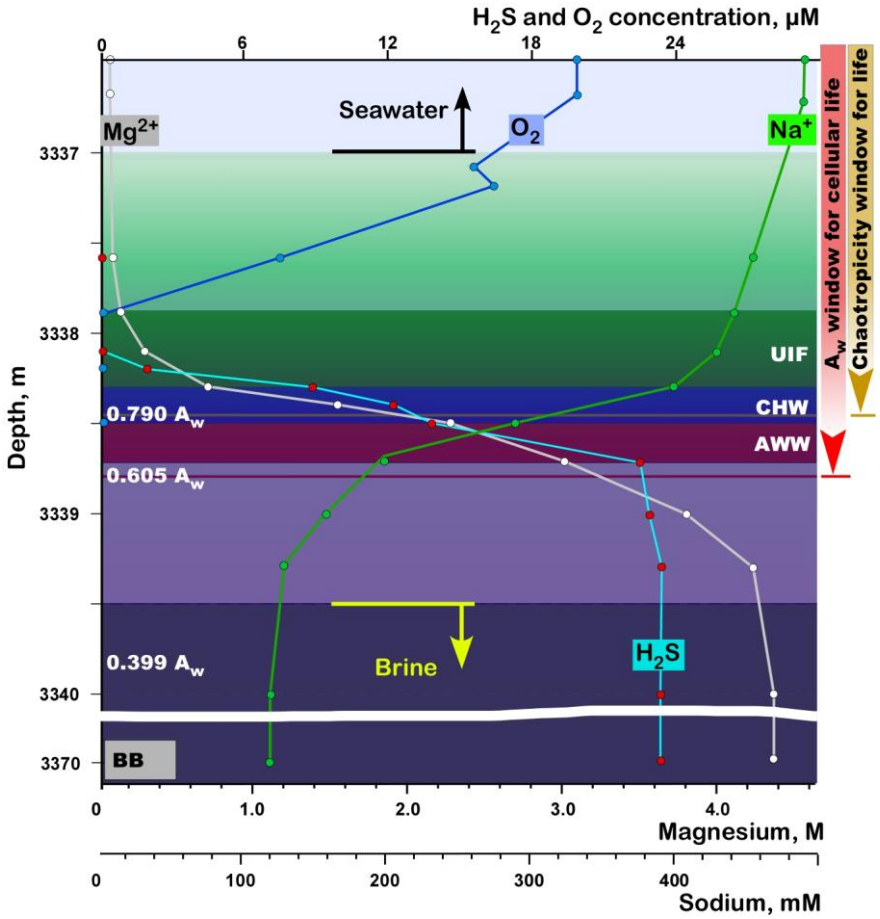

2

3 emi_12587_f3

4

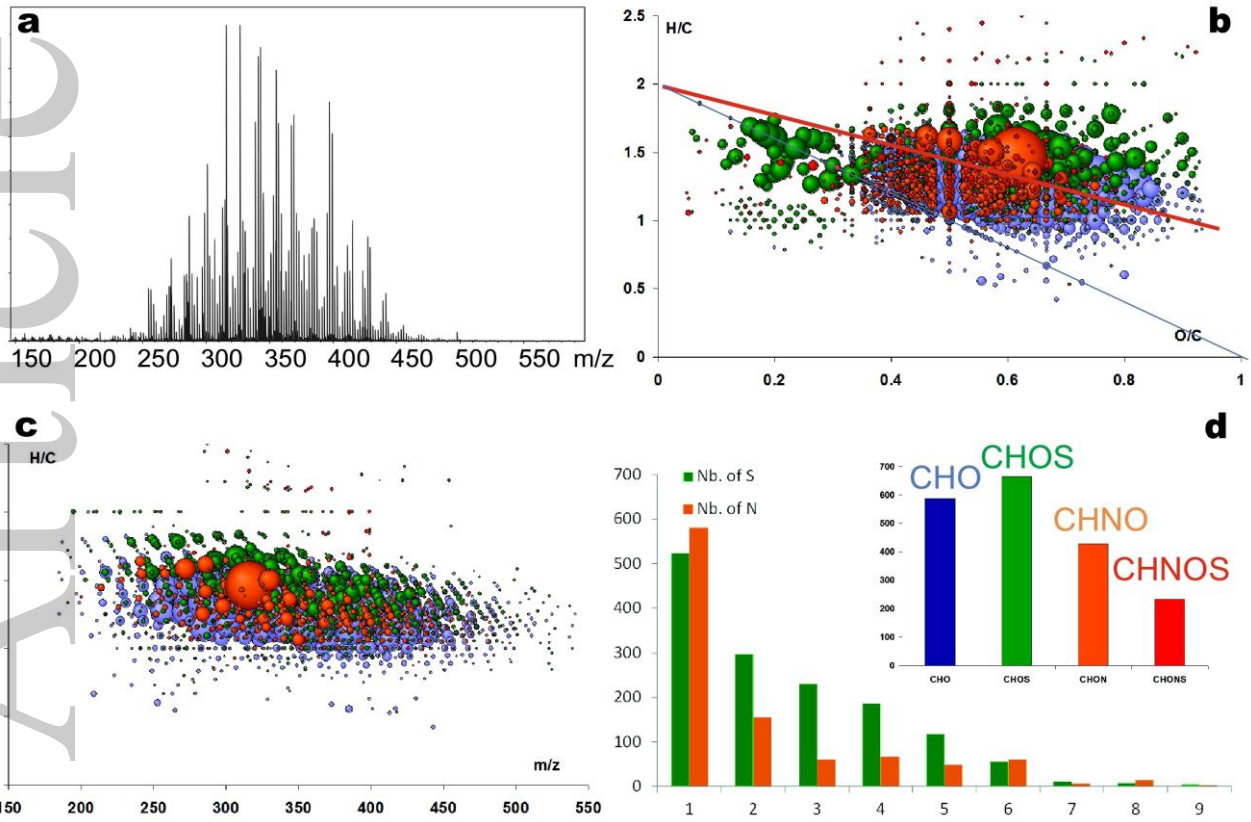

emi_12587_f4

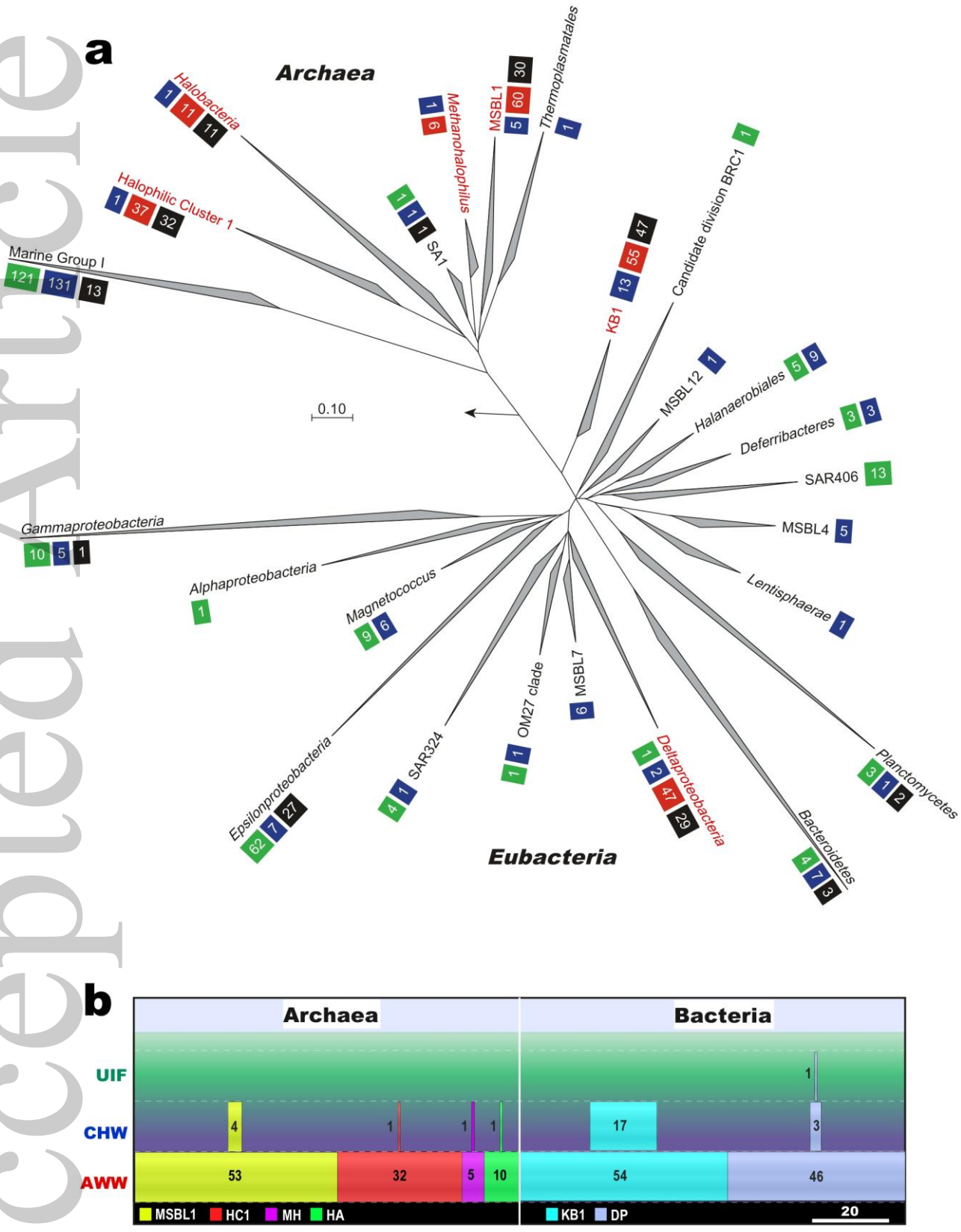

emi_12587_f5

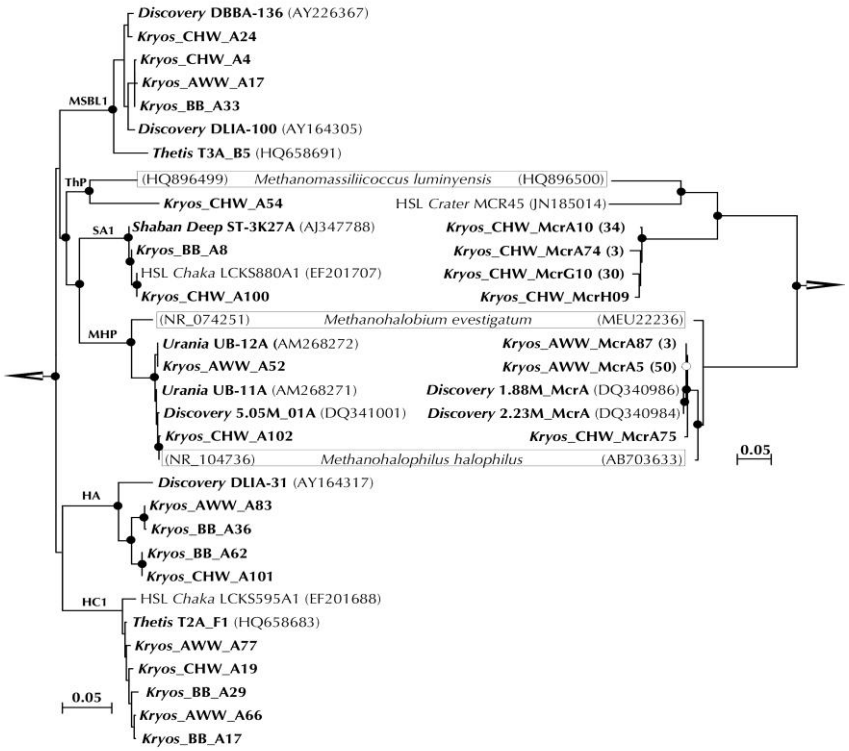

emi_12587_f6

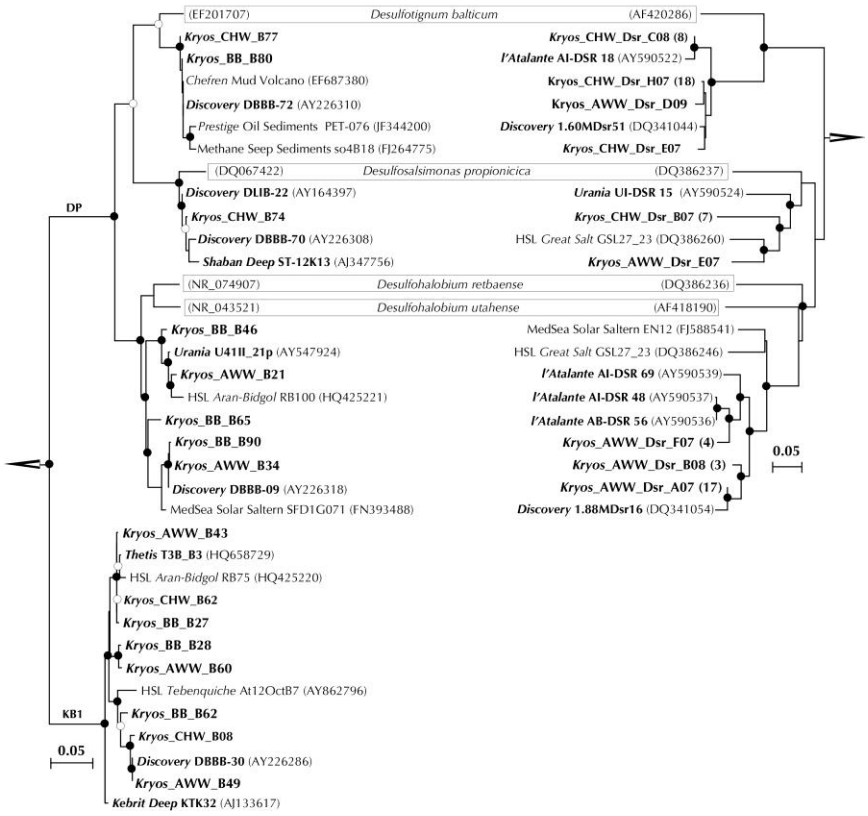

emi_12587_f7